The Effects of Circulating Antigen on the Pharmacokinetics and Radioimmunoscintigraphic Properties of ^{99m}Tc Labelled Monoclonal Antibodies in Cancer Patients

S.A. McQuarrie
Faculty of Pharmacy and Pharmaceutical Sciences, University of Alberta, Edmonton, Canada

T. Riauka
Faculty of Medicine, University of Alberta, Edmonton, Canada

R.P. Baum
Bad Berka PET Centre, Bad Berka, Germany

T.R. Sykes, A.A. Noujaim
AltaRex Inc., Edmonton, Canada

G. Boniface, G.D. MacLean
Biomira Inc., Edmonton, Canada

A.J.B. McEwan
Oncologic Imaging, Cross Cancer Institute, Edmonton, Canada

ABSTRACT **Purpose**. This article reports the pharmacokinetics, radiation dosimetry and radioimmunoscintigraphy (RIS) of two ^{99m}Tc-labelled monoclonal antibodies (MAb) used to detect cancer. **Methods**: The effects of circulating antigen in female cancer patients are explored and their effects on the ability of these MAbs to effectively perform as RIS agents noted. To illustrate the effects of circulating antigen, data using MAb B43.13 (OVAREX, AltaRex Corp., Waltham, MA, USA) from a Pilot study in ovarian cancer patients are presented. The results from a Phase II study of MAb 170H.82 (Tru-Scint AD, BIOMIRA INC., Edmonton, Alberta, Canada) in patients with primary and locally recurrent breast cancer were used to portray the biodistribution patterns when no circulating antigen is present. Data from planar gamma camera images were obtained for both groups and used for pharmacokinetic and radiation dosimetry analyses. **Results**: A pharmacokinetic analysis indicated a shorter residence time and higher clearance of ^{99m}Tc-MAb-B43.13 that was ascribed in part to the circulating CA 125 antigen in this group of ovarian cancer patients. **Conclusion**: These clearance patterns resulted in acceptable, though higher radiation doses to the spleen and urinary bladder wall for these patients when compared to the MAb-170H.82 group. Both MAbs were found to produce acceptable radioimmunoscintigraphic images.

Corresponding author: Dr. Steve McQuarrie, Faculty of Pharmacy & Pharmaceutical Sciences, University of Alberta, Canada, T6G 2N8.
email:smcquarrie@pharmacy.ualberta.ca

Key Words: pharmacokinetics - radiation dosimetry - technetium-99m – image processing - monoclonal antibodies - cancer

INTRODUCTION

Monoclonal antibodies (MAbs), labelled with appropriate radionuclides, have been extensively tested throughout the last decade as radioimmunoscintigraphy (RIS) agents in diagnostic oncology (1,2). Despite the promise held out by MAbs as highly specific targeting agents, and

encouraging preliminary results (3), the most are still in clinical trials and only a few MAb products are available commercially. The reasons behind their lack performance are varied (4, 5, 6, 7) and include: 1) low tumor uptake, 2) poor specificity and selectivity, 3) unwanted reactions with the immune system (human anti-mouse antibody or HAMA response), 4) effects of circulating antigen and 5) immunoconjugate stability (8). However, in spite of these problems, RIS techniques have not been abandoned, as several second-generation MAbs or MAb fragments have recently been approved or are nearing market approval (9). MAb-based products continue to be developed to take advantage of their targeting abilities for diagnosis and therapy (10, 11).

The importance of finding new tools in the diagnostic arsenal against breast cancer is evident from a recent study that has shown that breast cancer continues to be the most common cancer in women. In 1994 it was predicted that 182,000 new cases of breast cancer would occur in the United States, associated with an estimated 46,000 attributed deaths (12). Over the last three decades, increased 5-year survival has been ascribed to a number of causes including earlier detection and the implementation of adjuvant therapies. Current strategies utilized to provide early detection of breast cancers include breast self-examination, physician examination, and mammography with needle localization of specific mammographic abnormalities (13). Ovarian cancer is the second most common gynaecological malignancy and, despite recent improvements in diagnosis and treatment, it remains the leading cause of death in patients with gynaecological malignancies. The overall cure rate is approximately 37%. However, whilst 80 - 90% of those patients with local disease at presentation are cured, only 15 - 25% of those in whom the disease is disseminated may be cured (14).

Two second-generation MAbs used in the diagnosis of breast or ovarian cancer were compared in this study to analyze the effects of circulating antigen. The RIS and biodistribution patterns of ^{99m}Tc labelled MAb-B43.13 (ovarian cancer) and MAb-170H.82 (breast cancer) are described in this paper. A comparison of patient radiation dose estimates for these two ^{99m}Tc labelled MAbs are also presented. The effects of circulating antigen is explored in relation to the pharmacokinetics and the MAb's ability to effectively act as an RIS agent for these cancers.

Data for this study were obtained from two sources. As part of a pilot clinical study at the Johann Wolfgang Goethe University Medical Centre in Frankfurt, Germany, a radiopharmacokinetic model was developed to define the behavior of ^{99m}Tc-MAb-B43.13 for future diagnostic - and possible radioimmunotherapeutic trials (15). All patients enrolled in the trial had measurable levels of circulating antigen, CA 125. CA 125 is a high molecular weight glycoprotein associated with epithelial ovarian cancer and is widely used as a serum marker in this group of patients (16, 17) and in patients who have disseminated malignancy. It has been shown to be an effective marker of disease extent and of response to therapy. To illustrate the effects of no circulating antigen, results from a Phase II study using ^{99m}Tc-MAb-170H.82, in patients with primary and locally recurrent breast cancer at the Cross Cancer Institute in Edmonton (18) were used).

MATERIALS AND METHODS

Monoclonal Antibodies

MAb-B43.13 specifically recognizes CA 125. B43.13 is a murine IgG1, kappa light chain MAb with an affinity for CA 125 of approximately 1.2×10^9 M^{-1}. The MAb is supplied as a vial containing 2 mg of predispensed, sterile and non-pyrogenic frozen solution of derivatized MAb-B43.13 in the presence of saline and a buffer complex. The MAb was formulated using a photoactivation process (19). Labelling was performed with the addition of sodium pertechnetate ^{99m}Tc USP (1.6 - 2.0 GBq) to directly label the reduced thiol-groups to produce a nearly neutral pH solution that remained stable for at least two hours after radiolabelling. The radiochemical purity (percentage of ^{99m}Tc bound to MAb-B43.13) of the preparation was determined by instant thin layer chromatography (methanol:saline, 85:15). The product contained no antimicrobial preservative.

Approximately 5 mL of normal saline containing 2 mg of ^{99m}Tc-MAb-B43.13 was infused IV to each patient over a period of 1 minute.

The monoclonal antibody, MAb-170H.82 (IgG1 kappa light chain), was derived from a fusion between lymphocytes of balb/c mice immunized with a synthetic conjugate of the Thomsen Friedenreich antigen (20) and human serum albumin (TFβ/HSA), and fused to the fusion partner FOX/NY myeloma. In immunohistochemical studies this MAb strongly stains neoplastic cells derived from epithelial origins, including breast adenocarcinoma (21). Preliminary results suggest that the antigen to which MAb-170H.82 binds, is a membrane-associated glycoprotein of 35 kDa. Biomira Inc. (Edmonton, Alberta) supplied the MAb in kit form as a frozen liquid formulation (Tru-Scint © AD™). Radiolabelling was performed by the addition of sodium pertechnetate ^{99m}Tc USP, containing up to a maximum of 4,000 MBq in a maximum volume of 2 mL, to the vial containing the MAb. Dosages ranged from 1 to 4 mg of MAb in 5 mL of normal saline that was infused IV to each patient over a period of 1 minute. The radiochemical purity (percentage of ^{99m}Tc bound to MAb-170H.82) of the preparation was determined by instant thin layer chromatography (methanol:saline, 85:15). The product contained no antimicrobial preservative.

Patient Population

Fifty-three patients were enrolled into the MAb-170H.82 trial; the local ethics committee had approved the protocol and all patients gave written informed consent. The mean age was 51.4 years (range: 33 - 75). Patients included in this study had primary (n = 15) or metastatic adenocarcinoma (n = 38) of the breast and had undergone radiological evaluation of their tumor sites within 4 weeks of antibody injection. The tumor status of each patient at the time of participation was defined and compared with imaging results. Patients were excluded from the study if they had a prior history of significant allergic reactions. Following approval by the local ethics committee, a subgroup of six patients volunteered for the pharmacokinetic and radiation dosimetry study.

Ten patients were enrolled into the MAb-B43.13 study; the local ethics committee had approved the study and all patients gave written informed consent. All patients had been diagnosed with ovarian cancer, had previously undergone surgery and had failed to respond to one or more courses of chemotherapy. All patients had confirmed disease at the time of imaging. The age ranged from 24 to 72 years (mean age 55 years).

Imaging Parameters

Whole-body conjugate-view images were acquired with a dual-head gamma camera using a LEAP collimator. MAb-170H.82 was imaged with a Siemens camera (Siemens Medical Systems, Inc., Nuclear Medicine Group, Hoffman Estates, Illinois, USA) and MAb-B43.13 with a Picker camera (Picker International, Inc., Cleveland, Ohio, USA). Anterior and posterior whole body images for both studies were obtained immediately after injection and at 2-6, 14-18, 22-26 and 46 – 50 hours post injection.

Image Processing

Regions of interest (ROI) were chosen on the basis of observed organ uptake and the same ROIs were applied to all time points for a given patient, on both anterior and posterior projections. The unprocessed data recorded from the gamma camera consisted of 1) the number of counts in each ROI for the anterior and posterior images (heart, liver, spleen and left kidney), 2) the time required to acquire the image and 3) the elapsed time (post-injection). The geometric mean was calculated for each ROI from the anterior and posterior image data, corrected for the attenuation and scatter of gamma photons in tissue (22, 23) and decay corrected to the time of injection. Attenuation correction was estimated based on patient CT data, or if not available, from the mean of several patients within the study. The processed ROI counts were expressed as a percentage of the whole body, where the “immediate” whole-body image was assumed to represent 100% of the injected dose. The area under the time-activity-curve was used to estimate the cumulated activity for each ROI and, using standard MIRD schema (24) organ and whole-body radiation

doses were calculated. Tumor uptake was not calculated for either group as all of the patients in the B43.13 group had undergone prior surgery.

Data Processing

All data collation, data processing and radiation dose estimates were performed using programs developed with the spreadsheet program, Quattro Pro for Windows (Novell Inc. Release 6.0). S-values, used in radiation dosimetry calculations, were obtained from MIRDOSE2 (Copyright 1984, Oak Ridge Associated Universities, EE Watson, M Stabin and WE Bolch). Pharmacokinetic analyses for both the image and blood data were performed using a nonlinear least-squares regression program WinNonlin (Scientific Software Inc., Version 1.1). The program LAGRAN (25) was used to integrate the area under the ROI time-activity curve. Statistical analyses were performed using SPSS for Windows (SPSS Inc. Release 6.1). Gamma camera region-of-interest (ROI) data was calculated using Siemens software (B43.13) or MEDisplay (C-soft).

Biological Sampling

Serum data were collected from each patient at predetermined times up to 72 hours post-injection (approximately 0.25, 1, 2, 4, 6, 20, 26, 48 and 72h) and assayed for total radioactivity. In order to measure the stability of the ^{99m}Tc label in the patient's serum, an ELISA-based analysis of the MAb-B43.13 and SE-HPLC-based analysis of MAb-170H.82 was used (26). CA 125 levels were measured for the ovarian cancer group (ELISA). HAMA responses were tested for all patients in both studies. No adverse reactions to the radiolabelled MAb were seen in any patient. No clinically significant changes were determined between the pre-injection and post-injection haematological and biochemical parameters evaluated and there were no observed changes in vital signs following the administration of the radiolabelled MAb. Urine was collected from all patients at 6-hour intervals up to 72 hours post-injection.

RESULTS

Imaging

^{99m}Tc-MAb-170H.82

Fifty-one of the 53 patients enrolled were evaluable for assessment of efficacy. Two patients were considered non-evaluable; in one no disease was found at surgery despite a highly suspicious mammogram and biopsy; in the second patient the images were technically flawed and clinically uninterpretable. On a per patient basis RIS showed both sensitivity and positive predictive values of 96% (18).

Eighty-six lesions were scored as true positive in the total patient population. Twenty-nine of the lesions were seen only on SPECT imaging and 40 were delineated better on SPECT than on planar imaging, particularly in the axilla and in small lesions (< 1.5 cm) in the breast. Our RIS image data are presented in both static figures suitable for producing hard copy (suitable for a post-script based printout such as Adobe Acrobat^{TM}), or they can be observed in dynamic form using a suitable web-based browser. Figure 1 shows planar images of uptake in a primary breast cancer while Figure 2 and Figure 3 demonstrate the SPECT appearance of uptake in a primary tumor. ^{99m}Tc-MAb-170 was used successfully in identifying metastatic breast adenocarcinoma in various lymph node groups. Metastases were visualized in the axillary, internal mammary chain, and supraclavicular fossae lymph nodes. Examples of axillary and supraclavicular metastases identified are shown for planar (Figure 4) and SPECT (Figure 5) images**.** On-line manipulation of these images by the reader is possible when using Internet Explorer 4.0 or greater of Netscape 4.0 or greater. A Help file can be accessed to assist the reader in viewing these images.

Sensitivity and positive predictive accuracy data are reviewed elsewhere (18) it was not considered valid to calculate specificity, negative predictive value or accuracy as the patient population selection was based on a high probability of malignant disease. No

difference in sensitivity was seen among any of the three dose levels investigated and the same range of lesion size was found at all dose levels. The smallest soft tissue lesion detected was 0.5 cm and the largest was 7 cm. One lesion of 5 cm was not demonstrated. There was no correlation between size of lesion and true positivity.

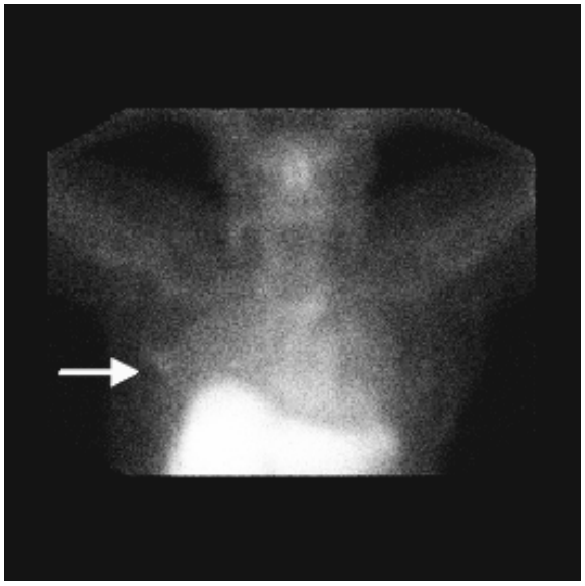

Figure 1: Planar gamma camera image illustrating the uptake of ^{99m}Tc-MAb-170H.82 in primary breast cancer.

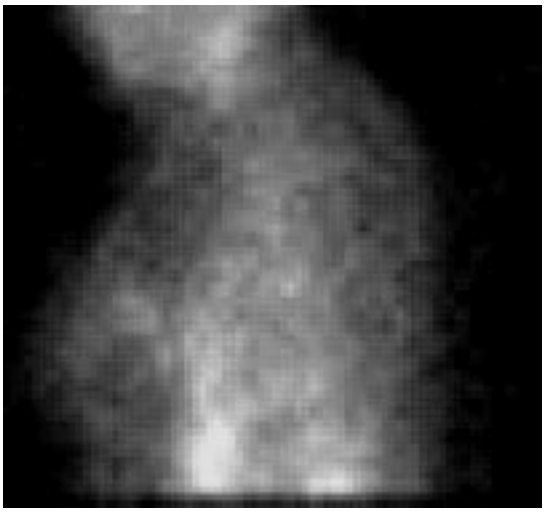

Figure 2: Image of the uptake of ^{99m}Tc-MAb-170H.82 in primary breast cancer. SPECT slices show breast tumor uptake of Tc-99m MAb-170H.82 in the left breast (SPECT slices 16 to 22 - increase intensity as needed). This uptake corresponds to a known lesion.

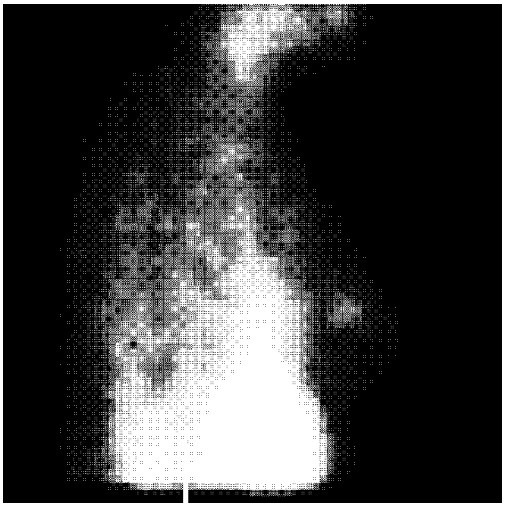

Figure 3: Image shows breast tumor uptake of Tc-99m MAb-170H.82 in the right breast corresponding to the known lesion.

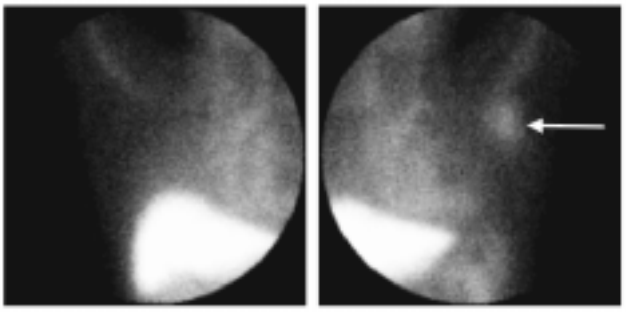

Figure 4: Planar image of the uptake of ^{99m}Tc-MAb-170H.82 in the left axilla at 24 hours post injection.

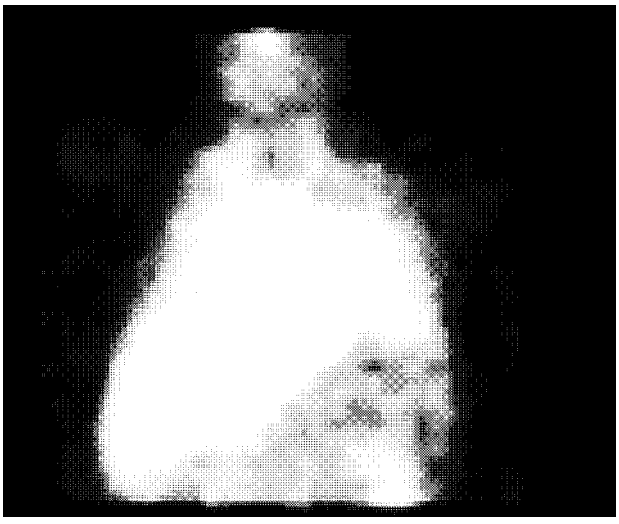

Figure 5: Image of the uptake of ^{99m}Tc-MAb-170H.82 in the right axilla.

In three patients, there was qualitative and quantitative increase in liver uptake at 24 hours (> 40% of the injected dose as determined by ROI analysis) and concomitant reduction in blood pool and lesion uptake. No relation to dose could be ascertained; liver function was normal in these patients and no hepatic metastases were demonstrated. HAMA was not present in any of the three patients. All three patients did poorly in their subsequent clinical course with rapidly progressive disease.

No meaningful difference among the three doses of MAb-170H.82 was observed, and the 1 mg dose has been chosen as the routine dose for all future imaging studies. No activity was seen at any time point in thyroid or stomach, confirming the absence of free ^{99m}Tc pertechnetate.

^{99m}Tc-MAb-B43.13

As this group of patients had previous surgery, no tumor assessment was made and the RIS data were used only to develop a pharmacokinetic model and provide radiation dosimetry estimates. Images were comparable to those described in the literature for ^{99m}Tc labelled antibodies (18, 27).

Pharmacokinetics

A two-compartment model was found to best represent the serum biodistribution of both ^{99m}Tc-labelled compounds. This model is be described by:

$$C(t) = C_1 e^{-\lambda_1 t} + C_z e^{-\lambda_z t} \qquad (1)$$

where: C_1 and C_Z are constants defined by the model and reflect the amount of product in each phase, λ_1 is the distribution phase rate-constant and λ_Z is the terminal elimination phase rate-constant. The volume of distribution for all data sets was approximately equal to the blood volume, within experimental error. Serum data used in development of this model are presented graphically for both MAbs in Figure 6, where the data points are estimated to have an associated error of 5%. A non-linear best-fit of the data was performed using WinNonlin.

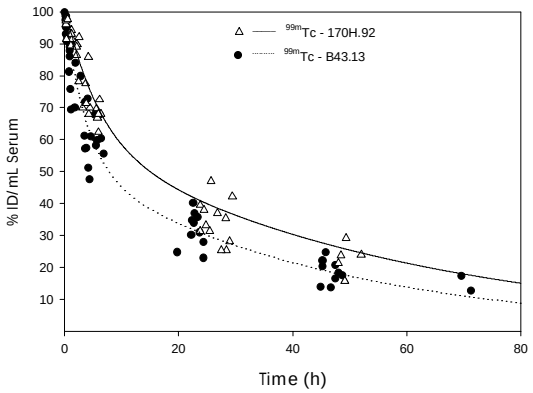

Figure 6: Serum biodistribution of 99mTc-MAb-B43.13 and 99mTc-MAb-170H.82. Solid and dotted lines represent the pharmacokinetic equations describing the biodistribution for each MAb.

A summary of the parameters representing coefficients from equation 1 (mean ± standard deviation), the ^{99m}Tc serum mean residence time (MRT) and the serum and renal clearance are presented in Table 1 (with estimates of the standard error). Half-lives are reported rather than the rate-constants to facilitate comparison with similar data in the literature, where $t_{½1}$ is the distribution phase half-life, and $t_{½Z}$ is the terminal elimination phase half-life.

The data were compared using equal- and unequal-variance t values, as well as a test for equality of variances and a 95% confidence interval for the difference in means. Homogeneity-of-variance was conducted using Levene's test that is less dependent on the assumption of normality than most tests.

Table: Mean pharmacokinetic parameters obtained from a two compartment model representing the biodistribution of ^{99m}Tc-MAb-B43.13 (n = 10) and ^{99m}Tc-MAb-170H.82 (n = 6), where: C_1 and C_Z are constants defined by the model, $t_{½1}$ is the distribution phase rate-half-life, $t_{½Z}$ is the elimination phase half-life and MRT is the mean residence time.

MAb	C_1(% ID)	C_z(% ID)	$t_{½1}$(h)	$t_{½Z}$(h)	MRT(h)	Serum Clearance (mL/h)	Renal Clearance (mL/h)
B43.13	48 ± 8	52 ± 8	2.6 ± 1.3	31.3 ± 4.8	42.1 ± 6.1	121 ± 33	53 ± 22
170H.82	42 ± 12	59 ± 10	4.4 ± 1.0	38.0 ± 4.8	50.1 ± 7.5	76 ± 20	31 ± 10
t-test (95%)	0.299	0.127	0.014	0.021	0.021	0.010	0.036

Only t_Z failed the Levene's test, in which case the unequal variance t-value was used. Equal variance t-values were used for all other variables. Significance values for the t-test are presented in the final row.

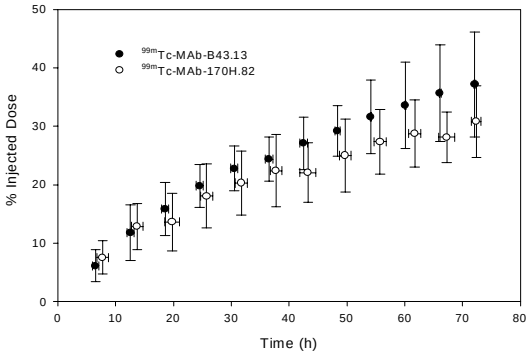

Figure 7: Urinary elimination of 99mTc labelled metabolites following the injection of 99mTc-MAb-B43.13 or 99mTc-MAb-170H.82 in patients expressed as a percentage of the injected dose (%ID).

In order to assess whether the model developed from radioactivity measurements reflected the distribution of the MAbs, an ELSIA-based test (for MAb-B43.13) and SE-HPLC methods (for MAb-170H.82) were used. A pharmacokinetic assessment of ^{99m}Tc-MAB-B43.13 was performed for both the radiolabelled compound and the intact MAb-B43.13 and are reported elsewhere. Both data sets were best fit by the same two-compartment model. Significant differences in the model constants, C_1 and Cz were found and indicated that there was a higher proportion of MAb-B43.13 in the elimination phase: C_1 (^{99m}Tc) = 48±8, C_1 (B43.13) = 28±18; Cz (^{99m}Tc) = 52±8, C_1(B43.13) = 72±18. No significant differences were found in any of the other model parameters. Only limited data were available to assess the biodistribution of ^{99m}Tc-MAb-170H.82 and MAb-170H.82. SE-HPLC was used to estimate the molecular weight of the radiolabelled compound in patient blood samples collected at 1 hour and 18 hours post-injection. Only radiolabelled MAb-170H.82 was present in the one hour sample, however approximately 8% of the radioactivity for the 18 hour sample was associated with an unidentified, low molecular weight compound, the remainder was associated with the intact MAb.

Dosimetry

Standard MIRD schema were used to estimate the radiation dose to patients receiving the ^{99m}Tc-labelled MAbs. Source organs were chosen from whole-body gamma camera images and ROIs were drawn around each organ and used to develop their respective time-activity curves**.** As no thyroid or bowel activity was observed, the contribution of unbound ^{99m}Tc was assumed to be negligible. Radiation dose estimates based on thyroid and bowel radioactivity were consequently deemed unnecessary. Tumors were not identified as part of this imaging protocol and as a result estimates of tumor uptake were not available. The radiation dose was calculated using, as source organs: the liver, spleen, kidneys, heart, the 'remainder of the body', and a dynamic bladder model.

Table: Radiation dose estimates expressed in mGy/GBq following the IV administration of ^{99m}Tc-MAb-B43.13 or ^{99m}Tc-MAb-170H.82.

Target Organs	Dose mGy/GBq		Target Organs	Dose mGy/GBq	
	B43.13	170H.82		B43.13	170H.82
Adrenals	13 ± 2	12 ± 0.6	Muscle	7 ± 1	6 ± 0.3
Brain	5 ± 1	5 ±0.3	Ovaries	10 ± 1	9 ± 0.5
Breasts	6 ± 1	5 ± 0.3	Pancreas	13 ± 2	11 ± 0.6
GB Wall	15 ± 3	14 ± 0.9	Red Marrow	8 ± 1	7 ± 0.4
LLI	9 ± 1	8 ± 0.5	Bone Surface	12 ± 2	11 ± 0.6
Sml Intestine	10 ± 1	9 ± 0.5	Skin	4 ± 1	4 ± 0.2
Stomach	10 ± 1	9 ± 0.4	Spleen	24 ± 11	9 ± 0.4
ULI	10 ± 1	9 ± 0.5	Thymus	9 ± 1	9 ± 0.6
Heart Wall	24 ± 4	26 ± 3.5	Thyroid	7 ± 1	6 ± 0.4
Kidney	38 ± 15	37 ± 6.9	UB Wall	31 ± 6	23 ± 6.5
Liver	29 ± 9	27 ± 3.2	Uterus	11 ± 1	9 ± 0.8
Lungs	9 ± 1	9 ± 0.5	Total Body	8 ± 1	7 ± 0.4

LLI = large lower intestine, ULI = upper large intestine, UB wall = urinary bladder wall

The main route of elimination was via the urinary system, where approximately 18% of the injected dose was eliminated in 24 hours. Kidney doses were estimated directly from gamma camera images as described above, however, due to the variable filling and voiding of the radioactive bladder contents, a mathematical model was used to evaluate the dose to the bladder wall. Dose estimates to the bladder wall in this report were based on the standard MIRD phantom (28, 29). As this model utilizes blood clearance in the determination of bladder wall dose, the urinary bladder dose was modified by the ratio of the urinary clearance to the blood clearance in order to compensate for elimination by other mechanisms, such as tissue uptake. Dosimetry estimates from these patient groups are presented in Table 2. Levene's test for equality of variances supported the assumption that the data were drawn from a homogeneous group so that equal-variance t-values were used for all comparisons. Significant differences were found for the spleen and urinary bladder wall ($p = 0.05$**)**.

DISCUSSION

Although the B43.13 and 170H.82 MAbs recognize different antigens, they are both of the same subclass (IgG1), and differ from each other only in the hyper-variable region. Both MAbs were labelled with ^{99m}Tc in the same manner. It was thus not unexpected that the same two-compartment model could be used to describe the serum biodistribution of both ^{99m}Tc labelled MAbs. However, significant differences were observed in the time-course of the two MAbs tested and are reflected in their elimination characteristics. MAb B43.13 was eliminated more quickly and was attributed to be due in part to the circulating CA 125. The effect of circulating CA 125 on the serum pharmacokinetics of this MAb has been previously evaluated (30), and no significant change in serum pharmacokinetics was observed over a wide range of CA 125 levels (up to 760 U/mL). However, it was observed that serum CA 125 levels were significantly reduced immediately post-injection, in most cases by over 90%. This implied almost complete antigen/antibody complex formation in the presence of the MAb-B43.13 excess and the subsequent rapid clearance of the complex from

circulation. These complexes are removed from the serum by the reticular endothelial system, of which the spleen is a likely organ contributing to their removal. Splenic uptake was confirmed on gamma camera images for the ^{99m}Tc-MAb-B43.13 group. This second route of clearance from the serum could help to explain its faster elimination properties when compared to MAb-170H.82, for which there was no associated circulating antigen. As no pre-existing HAMA response was observed for these groups of patients, the formation of a HAMA complex was not expected to significantly alter the observed pharmacokinetics.

Liver and kidney uptake for both MAbs was likely related to their metabolic and excretory functions, while one may speculate that the spleen localization observed for MAb-B43.13 may have an immunological basis. The urinary excretion value (approximately 18% at 24 hours) highlighted a further consequence of the study design, in that almost no immunoglobulin would be expected to be eliminated by this route during this time frame. This could be a result of the known metabolic handling of the ^{99m}Tc-immunoglobulin complex, during which there was dissociation of the radiolabel (31, 32). Although not measured, a contributing factor could be the metabolic removal of ^{99m}Tc from the MAb by transchelation to low molecular weight products, which are primarily cleared by the kidneys. This process is also supported by inherent instability in the ^{99m}Tc-MAb bond in the presence of endogenous sulphydryl containing substances (33, 34).

Tumor uptake as observed from the gamma camera images from these two RIS agents were not directly compared, as many of the ovarian cancer patients in the B43.13 trial had recent surgery to remove their primary tumor. The B43.13 imaging protocol was designed to collect data to establish the pharmacokinetic profile for this MAb and provided an estimate of the ^{99m}Tc radiation dosimetry. However, the imaging efficacy with MAb 170H.82 in breast cancer patients was measured prior to treatment and was found to detect tumor in both the primary site and in regional lymph nodes. These results, together with the sensitivity and positive predictive value reported elsewhere (18), suggests a possible clinical role for this MAb.

The low levels of HAMA seroconversion for these MAbs were lower than those reported in the literature (35, 36) suggesting that repeat imaging may be a possibility and that a wider routine role for this radiopharmaceutical could be envisaged, particularly in the ongoing management of this population of patients; multidose trials are required to confirm this. Adverse effects on serum tumor marker measurements are unlikely to occur in the presence of low HAMA, thus increasing the routine acceptability of the test (37).

Radiation dosimetry estimates obtained from this clinical trial are comparable to those quoted for other ^{99m}Tc labelled radiopharmaceuticals (38), and are significantly less than those reported for ^{111}In labelled Mabs (39). The administered dose of ^{99m}Tc used in this study is higher than in most routine nuclear medicine procedures; this dose was chosen to allow high quality SPECT images at 24 hours post injection and for dosimetry data acquisition to 48 hours. The estimates calculated for this paper appears to be in keeping with acceptable human limits, and comparable to most other diagnostic imaging investigations.

A visual inspection of the data in Table 2 describing the radiation dose estimates for the two ^{99m}Tc labelled MAbs revealed significant differences between two of the target organs; the urinary bladder wall and the spleen. An independent samples t-test yielded values of 0.025 for the bladder wall and 0.004 for the spleen at the 95% level of significance. One possible cause for the increased radiation dose to the spleen in the patient group receiving MAb-B43.13 could have been due to the effect of circulating CA 125, where the MAb/Ag complex was removed from the blood by the spleen. The higher radiation dose to the urinary bladder wall for ^{99m}Tc-B43.13 was attributed to the greater renal clearance observed for ^{99m}Tc-B43.13 (53 ± 22 mL/h) compared to ^{99m}Tc-170H.82 (31 ± 10 mL/h).

A comparison of these results to those of other directly ^{99m}Tc labelled immunoglobulins show no unusual accumulation and these MAbs appeared to behave in a relatively predictable and reproducible pattern within the limitations of the study (30, 40)

CONCLUSION

Although the B43.13 and 170H.82 MAbs are similar in that they are both from the same IgG1 subclass and were labelled with ^{99m}Tc in the same manner, their biodistribution patterns revealed that the ^{99m}Tc-MAb-B43.13 cleared more quickly. This was ascribed to complexation with the blood-borne CA 125 antigen, which was indirectly confirmed by the observed uptake in the spleen. RIS imaging did not appear to be compromised, and highlights the recognition of the native antigen *in vivo* by this MAb, and confirms its target specific localization capabilities reported as reported by Noujaim and co-workers (41). The pharmacokinetics for both of these MAbs facilitated RIS imaging and tumor visualization at 24 hours post-injection.

The Phase II RIS study from which the ^{99m}Tc-MAb-170H.82 patients were drawn has shown promise, and confirmed the results of the initial pilot study. A Phase III trial has commenced to evaluate the role of ^{99m}Tc-MAb-170H.82 in the workup of patients with locoregional recurrence. The pharmacokinetics and prior successful imaging with ^{99m}Tc-MAb-B43.13 in pilot studies suggest that further studies are justified for this agent as a diagnostic tool in the routine management of patients with ovarian cancer.

Radiation dose estimates for both MAbs were within expected ranges and posed no undue exposures within this group of patients.

ACKNOWLEDGEMENTS

Portions of this work were funded by a Medical Research Council of Canada Industry Award. The authors would also like to thank AltaRex Inc. (Edmonton, Canada) and Biomira Inc. (Edmonton, Canada) for their financial support and for supplying laboratory assistance and expertise. Mrs. Gail Amyotte and Mrs. Barbara Hornig provided valuable assistance in patient recruitment. We would also like to thank Mrs. Lori Golberg and Mr. Walter Korz for their assistance and expertise in the collection of patient data.

REFERENCES

1. Bodey B, Siegel SE, Kaiser HE. Human cancer detection and immunotherapy with conjugated and non-conjugated monoclonal antibodies. *Anticancer Research* 1996;16*(2):661*-74.
2. Divgi CR: - Status of radiolabeled monoclonal antibodies for diagnosis and therapy of cancer; *Oncology* 1996;10(6):939-953.
3. Britton KE, Granowska M. Immunoscintigraphy: Importance for researchers and patients; *Acta Oncologica* 1996;35(3):313-377.
4. Baquiran DC, Dantis L, McKerrow J: Monoclonal antibodies: innovations in diagnosis and therapy; *Seminars Oncol Nursing 1996;12(2):130-41* 130-411
5. Coons T; Monoclonal antibodies: the promise and the reality; *Radiologic Technology*.1995;67(1):39-60.
6. ain RK; Whitiker lecture: delivery of molecules, particles and cells to solid tumors; *Ann Biomed Eng* 1996;24:457-473.
7. Reilly RM, Sandhu J, Alvarez-Diez TM, Gallinger S, Kirsh J, Stern H. Problems of delivery of monoclonal antibodies. Pharmaceutical and pharmacokinetic solutions. *Clinical Pharmacokinetics*.1995;28(2):126-142.
8. Gooden,C.S.; Snook,D.E.; Maraveyas,A.; Rowlinson-Busza,G.; Peters,A.M.; Epenetos,A.A.; Direct technetium-99m labeling of three anticancer monoclonal antibodies: stability, pharmacokinetics and imaging; *J Nucl Med* 1995;36(5):842.-9
9. Biassoni L, D'Andrea V, Biancari F, Santoni F, Dibra A, De AE. Radiolabelled monoclonal antibodies in clinical and surgical oncology: a review; *Panminerva.Medica* 1997;39(1):46-52.
10. van,Gog FB; Visser,G.W.; Stroomer,J.W.; Roos,J.C.; Snow,G.B.; van,Dongen GA; High dose rhenium-186-labeling of monoclonal antibodies for clinical application: pitfalls and solutions, *Cancer* 1997 15;80(12 Suppl):2360.-70
11. White,C.A.; Halpern,S.E.; Parker,B.A.; Miller,R.A.; Hupf,H.B.; Shawler,D.L.; Collins,H.A.; Royston,I. Radioimmunotherapy of relapsed B-cell lymphoma with yttrium 90 anti-idiotype monoclonal antibodies. *Blood* 1996 ;87(9):3640.-9
12. Kelsey JL, Gammon MD. The epidemiology of breast cancer. *CA* 1991; 41:146-165.
13. Schmidt JG. The epidemiology of mass breast cancer screening -- a plea for a valid measure of benefit. *J Clin Epidemiol* 1990; 43:215-225.
14. Cohen CJ, Jennings TS. Screening for ovarian cancer: the role of noninvasive imaging techniques. *American J Obst Gynecol* 1994; 170(4):1088-94

15. Noujaim AA, Sykes TR, Madiyalakan R, Sykes CJ, Hertel A, Niesen A and Hör G; Monoclonal antibody B431.13 for immunoscintigraphy and immunotherapy of ovarian cancer, In Klapdor (ed) *Current Tumor Diagnosis: Applications, Clinical Relevance, Research, Trends Cancer of the Lung - State and Trends in diagnosis and Therapy*, W Zuckschwerdt Verlag. München, 1994 823-829.
16. Kenemans P, Yedema CA, Bon GG, von Mensdorff-Pouilly S. CA 125 in gynecological pathology--a review. [Review]. Eur J Obst, Gyn, Reprod Biol 1993;49(1-2):115-24.
17. Tuxen MK, Soletormost G, Dombernowsky P. Tumor markers in the management of patients with ovarian cancer. Cancer Treat Rev 1995;21(3):215-45
18. McQuarrie SA, MacLean GD, Boniface GR, Golberg K, McEwan AJB; Radioimmunoscintigraphy in Patients with Breast Adenocarcinoma Using ^{99m}Tc Labelled Monoclonal Antibody 170H.82 - Report of a Phase II Study, *Eur J Nucl Med*, 24:381-389, 1997.
19. Sykes TR, Woo TK, Baum RP, Qi P and Noujaim AA; Direct labeling of monoclonal antibodies with technetium-99m by photoactivation, J Nucl Med, 1995; 36:1913-1922.
20. Longenecker BM, Willans DJ, MacLean GD, Selvaraj S, Greenberg A, Suresh MR and Noujaim AA; Monoclonal antibodies and synthetic tumor associated glycoconjugates to study the expression of Thomsen-Friedenreich (TF)-like and Tn-like antigens on human cancers. *J Natl Cancer Inst* 1987; 78:489-496.
21. Samuel J, Noujaim AA, MacLean GD, et al. Analysis of human tumor associated Thomsen-Friedenreich antigen. *Cancer Res* 1990; 50:4801-4808.
22. Harris CC, Greer KL, Jaszczak RJ, Floyd Jr CE, Fearwow EC and Coleman RE; 99m-Tc attenuation coefficients in water-filled phantoms determined with gamma cameras. *Med Phys* 1984; 11: 687.
23. Bailey DL, Hutton BF and Walker PJ. Improved SPECT using simultaneous emission and transmission tomography. *J Nucl Med* 1987; 28: 844.
24. Loevinger R, Budinger TF and Watson EE. *MIRD Primer for Absorbed Dose Calculations*. New York, NY: Society of Nuclear Medicine, 1988.
25. Ediss C and Tam YK. An interactive program for determining areas bounded by drug concentration curves using lagrange interpolation. *J Pharmacol Toxicol Meth* 1995; 34: 165-168.
26. Muddukrishna SN, Jorge P, Machner w, Sykes TR and Noujaim AA; An improved method for analysis of technetium radiolabelled antibody by size-exclusion HPLC; *Appl J Radiat Isotopes*, 1994, 45:1009-1019.
27. S.A. McQuarrie, A.J.B. McEwan, A.A. Noujaim, R.P. Baum, A. Niesen, L. Golberg, K. Golberg, A Pharmacokinetic Comparison of Murine and Chimeric Forms of the ^{99m}Tc Labelled 174H.64 Monoclonal antibody, *J Nucl Biol and Med*, 1994;38(Suppl 1 to 4), 140-144.
28. Cloutier SR, Smith SA, Watson EE, et al. Dose to the fetus from radionuclides in the bladder. *Health Phys* 1973; 25:147-161.
29. Snyder WS, Ford MR and Warner GG; Estimates of Specific Absorbed Fractions for Photon Sources Uniformly Distributed in Various Organs of a Heterogeneous Phantom, MIRD Pamphlet No. 5, Revised; Society of Nuclear Medicine, New York, NY, 1978.
30. S.A. McQuarrie, R.P. Baum, A. Niesen, R. Madiyalakan, W. Korz, T.R. Sykes, C.J. Sykes, G Hör, A.J.B. McEwan, and A.A. Noujaim; Pharmacokinetics and Radiation Dosimetry of ^{99m}Tc Labelled Monoclonal Antibody B43.13 in Ovarian Cancer Patients, *Nucl Med Communications*, 1997, 18:878-886.
31. Xue LY, Noujaim AA, Sykes TR, Woo TK and Peng Z; Studies on Metabolism of directly labeled 99mTc-antibody in mice, *Quart J Nucl Med* 1997; 40:341-350
32. Xue LY, Noujaim AA, Sykes TR, Woo TK and Wang XB; Role of transchelation in the uptake of 99mTc antibodies in liver and kidney, *Quart J Nucl Med*, 1997; 41:10-17
33. Hnatowich DJ, Mardirossian G, Rusckowski M, Fogarasi M, Virzi F and Winnard Jr P; Directly and indirectly technetium-99m-labeled antibodies - a comparison in in vitro and animal in vivo properties, *J Nucl Med* 1993; 34:109-119.
34. Mardirossian G, Wu C, Ruskowski M and Hnatowich DJ; Stability of ^{99m}Tc directly labelled to a Fab' via stannous ion and mercaptoethanol, *Nucl Med Commun* 1992, 13:503-512.
35. van Krooneburgh MJPG, Pauwels EJK. Human immunological response to mouse monoclonal antibodies in the treatment or diagnosis of malignant disease. *Nucl Med Commun* 1988; 9:919-930.
36. Reynolds JC, Del Vecchio S, Sukahara H, Lora ME, Carrasuillo JA, Neuman RD and Larson SM; Anti-murine antibody response to mouse monoclonal antibodies: Clinical findings and implications. *Nucl Med Biol* 1989; 16:121-125.
37. Janssen JAMJL, Blankestijn PJ, Docter R, et al. Effects of immunoscintigraphy with monoclonal antibodies in assays of hormones and tumor marker. *Br Med J* 1989; 298:1511-1513.
38. Bischof Delaloye A and Delaloye B. Radiolabelled monoclonal antibodies in tumour imaging and therapy: out of fashion? *Eur J Nucl Med*, 1995; 22: 571-580.
39. McEwan AJB, MacLean GD, Hooper HR, et al. MAb 170H.82: an evaluation of a novel panadenocarcinoma monoclonal antibody labelled with ^{99m}Tc and with ^{111}In. *Nucl Med Commun* 1992; 13:11-19.
40. McQuarrie SA, McEwan AJB, Noujaim AA, Boniface GR, Golberg K, Golberg L and Sykes TR; Pharmacokinetics and radiation dosimetry of ^{99m}Tc labelled monoclonal antibody 170H.82 in breast cancer patients with no circulating antigen, *Quart J Nucl Med*, 1995, 39:36.
41. Noujaim AA, Sykes TR, Madiyalakan R, Sykes CJ, Hertel A, Niesen A and Hör G; Monoclonal antibody B431.13 for immunoscintigraphy and immunotherapy of ovarian cancer, In Klapdor (ed) *Current Tumor Diagnosis: Applications, Clinical Relevance, Research, Trends Cancer of the Lung - State and Trends in diagnosis and Therapy*, W Zuckschwerdt Verlag. München, 1994 823-829.